

NCC 2-327
IN-03-CR
030141

Comprehensive Analysis of Two Downburst-Related Aircraft Accidents

J. Shen, E. K. Parks, R. E. Bach

Reprinted from

Journal of Aircraft

Volume 33, Number 5, Pages 924-930



A publication of the
American Institute of Aeronautics and Astronautics, Inc.
1801 Alexander Bell Drive, Suite 500
Reston, VA 22091

Comprehensive Analysis of Two Downburst-Related Aircraft Accidents

J. Shen*

University of Texas at Austin, Austin, Texas 78723

E. K. Parks†

University of Arizona, Tucson, Arizona 85721

and

R. E. Bach‡

NASA Ames Research Center, Moffett Field, California 84035

Although downbursts have been identified as the major cause of a number of aircraft takeoff and landing accidents, only the 1985 Dallas/Fort Worth (DFW) and the more recent (July 1994) Charlotte, North Carolina, landing accidents provided sufficient onboard recorded data to perform a comprehensive analysis of the downburst phenomenon. The first step in the present analysis was the determination of the downburst wind components. Once the wind components and their gradients were determined, the degrading effect of the wind environment on the airplane's performance was calculated. This wind-shear-induced aircraft performance degradation, sometimes called the *F*-factor, was broken down into two components F_1 and F_2 , representing the effect of the horizontal wind gradient and the vertical wind velocity, respectively. In both the DFW and Charlotte cases, F_1 was found to be the dominant causal factor of the accident. Next, the aircraft in the two cases were mathematically modeled using the longitudinal equations of motion and the appropriate aerodynamic parameters. Based on the aircraft model and the determined winds, the aircraft response to the recorded pilot inputs showed good agreement with the onboard recordings. Finally, various landing abort strategies were studied. It was concluded that the most acceptable landing abort strategy from both an analytical and pilot's standpoint was to hold constant nose-up pitch attitude while operating at maximum engine thrust.

Nomenclature

a_x, a_y, a_z	= body-axis accelerations
C_L, C_D	= lift, drag coefficients
$C_{L\alpha}, C_{m\alpha}, C_{m\dot{\alpha}}$	= stability derivative
C_m	= pitching moment coefficient
$C_{y\beta}$	= side-force coefficient
D	= drag
F, F_1, F_2	= <i>F</i> -factor and its components
h, h_e	= geometric and energy altitude
I_{yy}	= moment of inertia about y axis
q	= pitch rate
T	= thrust
U, W	= body-axis velocity components
V	= true airspeed vector
W	= wind velocity vector
W_x, W_y, W_z	= north, east, and upward wind vector components
W_{xy}	= horizontal tailwind
x, y, h	= aircraft position (Earth frame)
α, α_{vane}	= angle of attack, vane angle
β	= side-slip angle
γ_a	= air mass flight-path angle
δ_{flap}	= flap deflection angle

δ_H	= stabilizer deflection angle
ψ_w	= wind-axis heading angle
ψ, θ, ϕ	= body-axis Euler angles

I. Introduction

WIND shear has been a major cause of aircraft accidents throughout aviation history. In the U.S., between 1964 and 1985, wind shear has contributed to at least 26 civil accidents involving more than 500 fatalities.¹ In the five years following 1986, airline pilots have reported 96 severe turbulence incidents,² some of them involving downbursts.

Two common types of airplane encounters with wind shear are turbulence encounters at high cruising altitudes and downburst penetrations during takeoff and landing. Downbursts occur near the ground beneath storm cells and may be accompanied by heavy rain (wet downbursts) or in some cases, if the atmosphere is very dry, may occur in the virga beneath the storm cell (dry downbursts).³ Downbursts can also be classified as microbursts or macrobursts according to the diameter of the outburst winds.³ Since the first recognized downburst accident in 1956, there have been at least eight other major encounters. A tabulation of downburst accidents/incidents is shown in Table 1.

Previously, in cases of clear air turbulence incidents, data from the onboard Digital Flight Data Recorder (DFDR) have been used in conjunction with ground-based radar tracking (ATC radar) to extract the components of the turbulent winds.⁴⁻⁶ Bach and Wingrove⁶ provided the wind estimations used in the preliminary investigation of the Delta L-1011 accident that occurred during landing at the Dallas/Fort Worth airport. Fujita⁷ performed DFW downburst studies. As previously mentioned, only two of the nine downburst accidents listed in Table 1 involved airplanes equipped with DFDRs, i.e.,

Received Aug. 28, 1995; presented as Paper 96-0895 at the AIAA 34th Aerospace Sciences Meeting and Exhibit, Reno, NV, Jan. 15–19, 1996; revision received May 6, 1996; accepted for publication May 14, 1996. Copyright © 1996 by the American Institute of Aeronautics and Astronautics, Inc. All rights reserved.

*Graduate Student. Student Member AIAA.

†Professor Emeritus, Department of Aerospace and Mechanical Engineering. Associate Fellow AIAA.

‡Aerospace Engineer, Guidance and Navigation Branch, M/S 210-9. Member AIAA.

Table 1 History of downburst accidents

Location	Date	Airplane	Takeoff/landing	Fatality/passenger
Kano, Nigeria	June 24, 1956	Boac Arogaut	Takeoff	32/45
Pago Pago, Somoa	January 30, 1974	Pan Am 806	Landing	96/101
JFK, New York	June 24, 1975	B-727 (Eastern 66)	Landing	112/124
Denver	August 7, 1975	Continental 426	Takeoff	0/134
Doha, Qatar	May 14, 1976	Royal Jordian 600	Landing	45/64
Philadelphia, PA	June 23, 1976	Allegheny 121	Takeoff	0/106
New Orleans, LA	July 9, 1982	B-727 (Pan Am 759)	Takeoff	152/161
Dallas Fort Worth, TX	August 2, 1985	L-1011	Landing	137/163
Charlotte, NC	July 2, 1994	DC-9	Landing	37/57

the DFW L-1011 landing accident in 1985 and the 1994 Charlotte, North Carolina DC-9 accident that occurred during an attempted landing abort. Thus, the lack of an adequate database restricted the present analysis to these two accidents.

This article analyzes in detail the two previously mentioned encounters. Wind components in both cases were estimated. The degradation of the aircraft's climb capability and ability to maintain airspeed, sometimes called the F -factor, was calculated and discussed. Also, flight simulations were performed to validate the aerodynamic model and to examine various landing abort strategies.

II. Wind Estimation Methods

Before the introduction of the flight data recorder (FDR) and the cockpit voice recorder (CVR), aviation accident investigators had to rely on examination of the wreckage, meteorological data, and interviews of survivors and eyewitnesses. This method left a lot of questions unanswered. The early FDRs recorded only four channels of data: 1) indicated airspeed, 2) vertical acceleration, 3) pressure altitude, and 4) magnetic heading, along with radio transmission times. Although an improvement in the investigation of the wind-shear-related accidents, the information provided was so sparse that investigators were unable to reconstruct, with any precision, the wind environment surrounding the accident (e.g., Eastern Airlines Fl-66, John F. Kennedy Airport, New York, and Pan Am Fl-759, New Orleans, Louisiana).

Digital flight data recorders were made mandatory on all large airliners certified after 1969. The extensive set of variables recorded on the DFDR along with ATC radar tracking data now provided a sufficient data set to accurately reconstruct the wind environment experienced by the airplane.^{4,5}

The wind vector W is defined as

$$W = V_t - V \quad (1)$$

where V_t is the aircraft velocity in an Earth-fixed frame, and V is the vector of the true airspeed relative to the moving air mass (Fig. 1). The three components of W are given by the following equations:

$$W_x = \dot{x} - V \cos \psi_w \cos \gamma_a \quad (2)$$

$$W_y = \dot{y} - V \sin \psi_w \cos \gamma_a \quad (3)$$

$$W_h = \dot{h} - V \sin \gamma_a \quad (4)$$

where γ_a , the air mass flight path angle, and ψ_w , the wind axis heading angle, are calculated from the following equations⁴:

$$\sin \gamma_a = \cos \alpha \cos \beta \sin \theta - C \cos \theta \quad (5)$$

$$\tan(\psi_w - \psi) = \frac{\sin \beta \cos \phi - \sin \alpha \cos \beta \sin \phi}{\cos \alpha \cos \beta \cos \theta + C \sin \theta} \quad (6)$$

$$C = \sin \alpha \cos \beta \cos \phi + \sin \beta \sin \phi \quad (7)$$

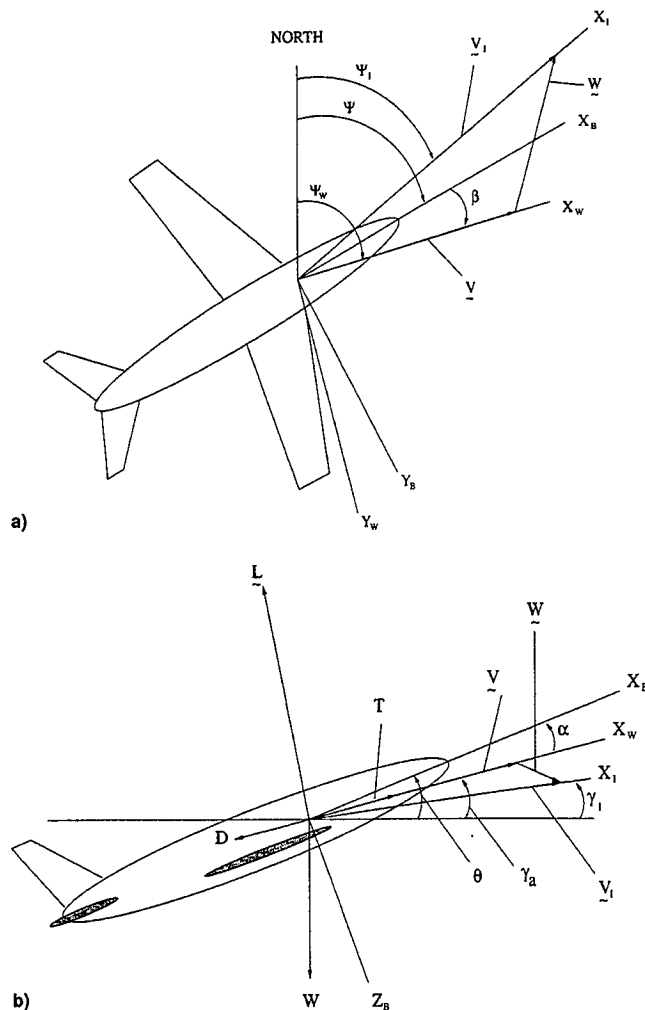


Fig. 1 Velocity vector: a) plan and b) side views.

The angle β is calculated using the following equation:

$$\beta = (1/C_{y\beta})(a_y C_w - C_{y\delta_r} \delta_r) \quad (8)$$

where C_w is the weight coefficient, $C_{y\beta}$ and $C_{y\delta_r}$ are side-force derivatives, and δ_r is the rudder-deflection angle.

The velocity components in an Earth-fixed coordinate system may be calculated, using the following equations⁸:

$$\dot{x} = a_x \cos \theta \cos \psi + a_y (\sin \phi \sin \theta \sin \psi - \cos \phi \sin \psi) + a_z (\cos \phi \sin \theta \cos \psi + \sin \phi \sin \psi) \quad (9)$$

$$\dot{y} = a_x \cos \theta \sin \psi + a_y (\sin \phi \sin \theta \sin \psi + \cos \phi \cos \psi) + a_z (\cos \phi \sin \theta \sin \psi - \sin \phi \cos \psi) \quad (10)$$

$$\dot{h} = a_x \sin \theta - (a_y \sin \phi + a_z \cos \phi) \cos \theta - 1 \quad (11)$$

These equations are integrated successively to provide the inertial velocities \dot{x} , \dot{y} , and \dot{h} and the inertial positions x , y , and h . Biases and initial conditions are determined by matching the calculated ground positions to ATC radar tracking data and the calculated altitude to the DFDR recorded barometric altitude.⁴⁻⁶

There are two methods of determining the angle of attack. In the DFW case, a direct measurement of the angle of attack was made with a vane. In this case, with a flap setting of 33 deg, the true α is given by the calibration equation:

$$\alpha = 0.535\alpha_{\text{vane}} + 3.72 \text{ deg} \quad (12)$$

In the Charlotte case, where no direct measurement of the angle of attack was made, the angle of attack was determined

from the lift curve (i.e., C_L vs α) at the specified flap setting using the following equations:

$$n_{zw} = -a_z \cos \alpha + a_x \sin \alpha \quad (13)$$

$$C_L = n_{zw}W/qS = n_{zw}C_w \quad (14)$$

$$\alpha = (C_L/C_{L\alpha}) + \alpha_0 \quad (15)$$

where n_{zw} is the wind-axis vertical load factor. In this case, when the pilot decided to abort the landing, the flaps of the DC-9 were retracted from 40 to 15 deg. In performing the calculation of α , since no recording of flap deflection was available, it was assumed that the flap retraction was started 15 s before ground impact and that the flap deflection decreased at a constant rate from 40 to 15 deg over a period of 11 s.

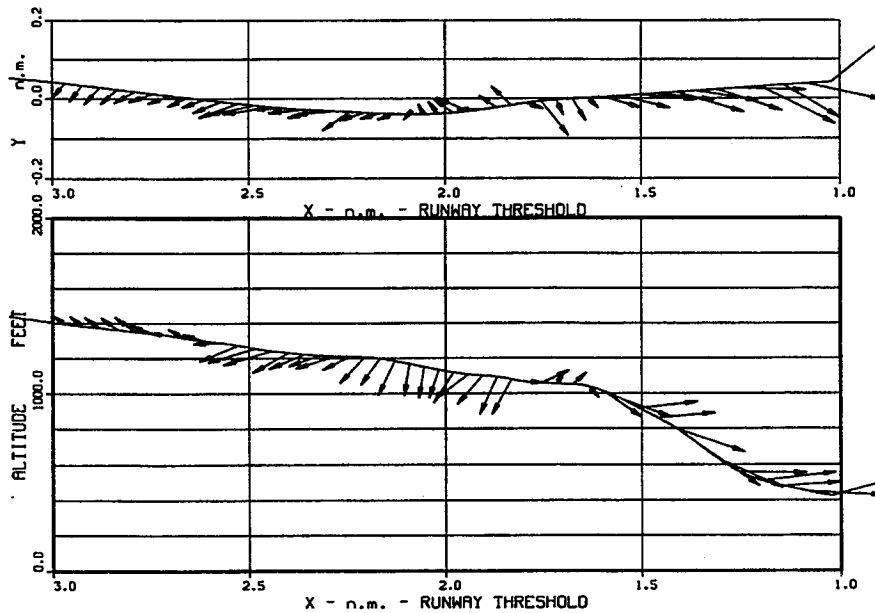


Fig. 2 DFW wind (1-s interval)

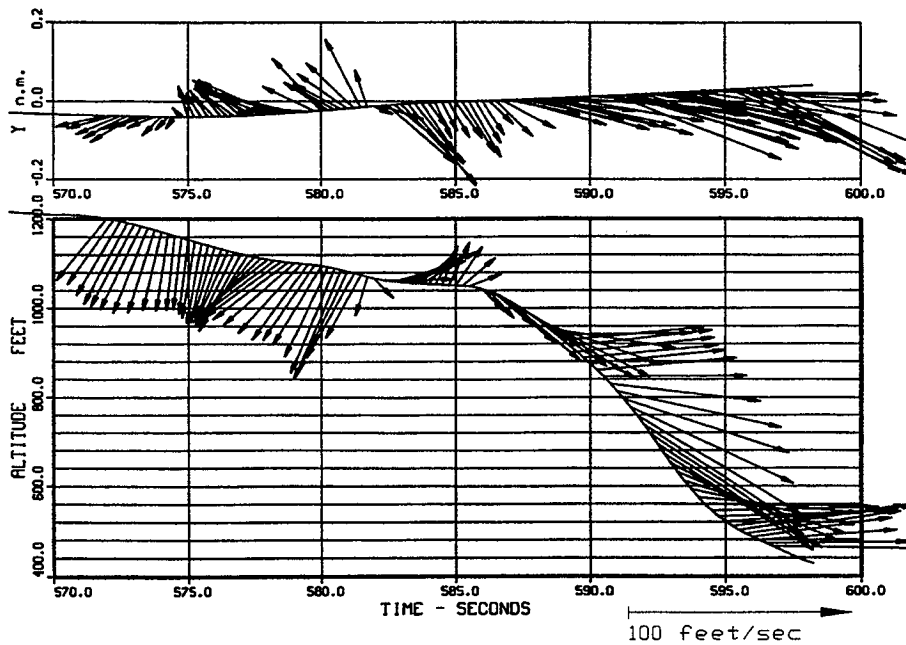


Fig. 3 DFW wind (1/4-s interval).

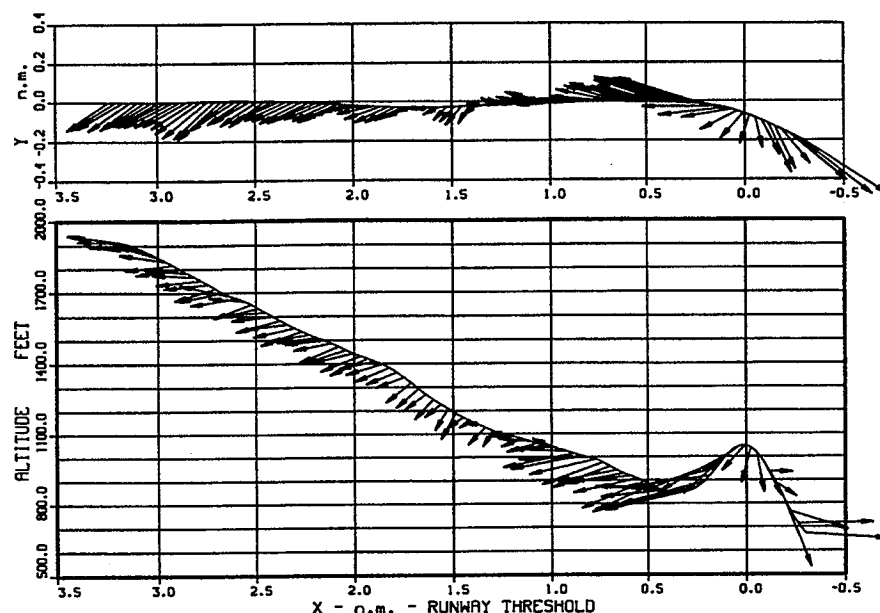


Fig. 4 Charlotte wind (1-s interval).

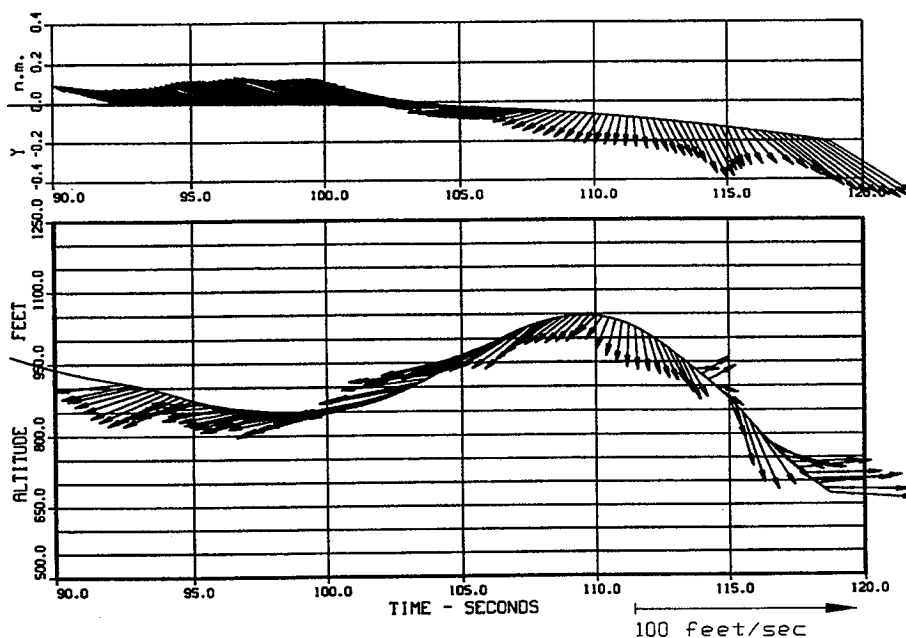


Fig. 5 Charlotte wind (1/4-s interval).

III. Derived Winds

Vector plots of the wind components for the DFW case are shown in Figs. 2 and 3 in both plan and elevation views. The Charlotte wind vectors are displayed in Figs. 4 and 5. As observed, during downburst encounters, the airplane, as it enters the downburst, first encounters strong headwinds that rapidly change into tailwinds. All the while, during the downburst penetration, the aircraft is subjected to downdrafts of variable intensity.

Entrained vortices are sometimes observed in downbursts. They occur near the ground in the outflow along the perimeter of the vertical column of the downburst. The vortices, depending on their strength, can be very damaging to the aircraft's performance. These entrained vortices can be seen in both the DFW and Charlotte cases. In the DFW case the vortex was sufficiently strong to cause the airplane to reach a stalling angle of attack as it exited the vortex. This vortex was encountered about 16 s before ground impact and was possibly

the major cause of the accident. After the vortex encounter the airplane never recaptured the glide slope or regained a suitable nose-up pitch attitude. In the Charlotte case, as shown in Figs. 4 and 5, the vortex was much smaller and less intense and played a minor role in the accident.

IV. Performance Degradation, F -Factor

The damaging effect of a downburst is based on the fact that when the aircraft enters a downburst it first gains airspeed as a result of the increasing headwind. This may prompt the pilot to intuitively decrease power. A few seconds later, the headwind decreases as the aircraft penetrates deeper into the downburst. As the airplane exits the core of the downburst, it is being pushed downward by strong vertical winds that are accompanied by large increases in tailwind. This sudden loss of airspeed and altitude places the aircraft in a precarious position with respect to maintaining the glide slope and a suitable flying speed.

To quantitatively analyze the aircraft performance capability, a quantity, h_e , called herein the energy height and defined as the total energy per unit weight, was used. Thus,

$$h_e = h + (V^2/2g) \quad (16)$$

where h is a measure of the potential energy and $V^2/2g$ represents the kinetic energy (V is the airspeed). The rate of the increase in total energy when subjected to horizontal and vertical winds, W_x and W_h is⁹

$$\dot{h}_e = \frac{(T - D)}{W} V - \left(\frac{\dot{W}_x}{g} - \frac{W_h}{V} \right) V \quad (17)$$

which, in dimensionless form becomes

$$\frac{\dot{h}_e}{V} = \frac{(T - D)}{W} - \left(\frac{\dot{W}_x}{g} - \frac{W_h}{V} \right) \quad (18)$$

where W is the airplane's weight.

$[(\dot{W}_x/g) - (W_h/V)]$ is a measure of the degradation of the aircraft performance capability, and is sometimes called the F -factor.¹ Thus,

$$F = (\dot{W}_x/V) - (W_h/V) \quad (19)$$

The F -factor may be broken down into components F_1 and F_2 , representing the effect of the changing headwinds and the downdrafts, respectively. Thus,

$$F_1 = \dot{W}_x/g \quad (20)$$

$$F_2 = -(W_h/V) \quad (21)$$

From the definition, it can be seen that the larger F becomes, the more restricted the airplane's climb performance will become. When the F -factor exceeds a certain value [e.g., $F > (T - D)/W$] over a certain finite time span, the airplane will be unable to maintain the energy level necessary to safely complete the landing or takeoff operation. The F -factor and its components for the two cases were calculated and are shown in Figs. 6-9. As one of the most severe downbursts ever documented, the DFW case had an F -factor reaching a value approaching 1.0 while traversing the core of entrained vortex. In the Charlotte case the downburst in terms of the F -factor is shown to be relatively less intense. It can be seen that, in both

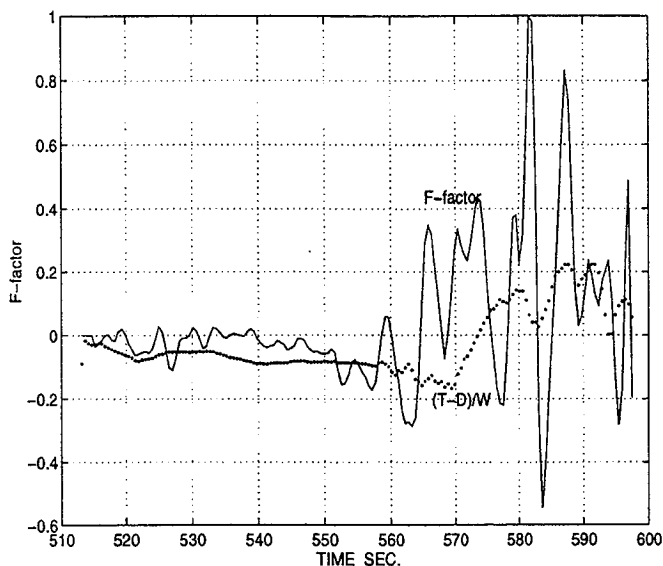


Fig. 6 DFW F -factor.

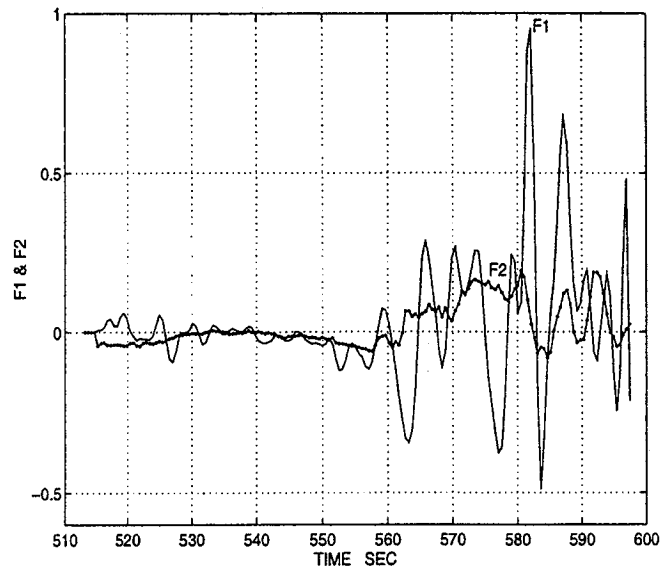


Fig. 7 DFW F -factor components.

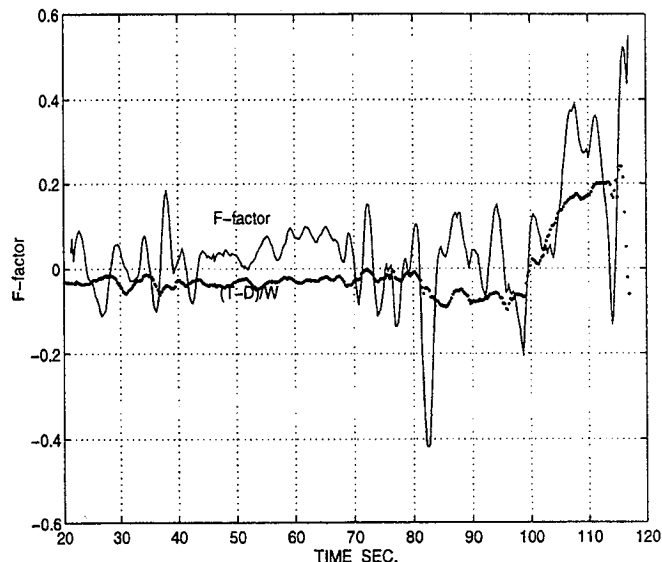


Fig. 8 Charlotte F -factor.

cases, F_1 is significantly larger than F_2 , indicating that the horizontal wind gradient was the dominant cause of the accidents.

V. Landing Abort Strategies

Various landing abort strategies were examined for both the DFW and Charlotte accidents. A three-degree-of-freedom longitudinal aerodynamic model was devised. The model was first validated by comparing the airplane's response to the winds and the recorded control inputs with the DFDR recorded outputs. The comparison showed good agreement.

A. Flight Simulation

The simulation assumed an Earth-based inertial frame and the aircraft as a rigid body. The linearized longitudinal equations of the airplane are⁸

$$\dot{U} = (1/m)X - g \sin \theta - qW \quad (22)$$

$$\dot{W} = (1/m)Z + g \cos \theta + qU \quad (23)$$

$$\dot{q} = M/I_{yy} \quad (24)$$

$$\dot{\theta} = q \quad (25)$$

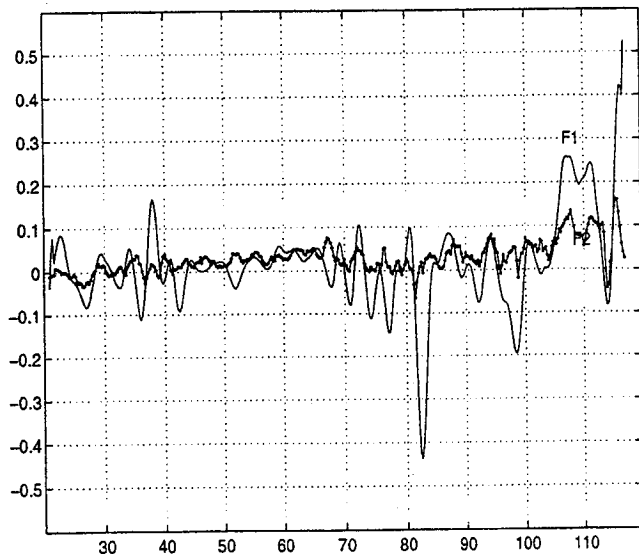


Fig. 9 Charlotte F-factor components.

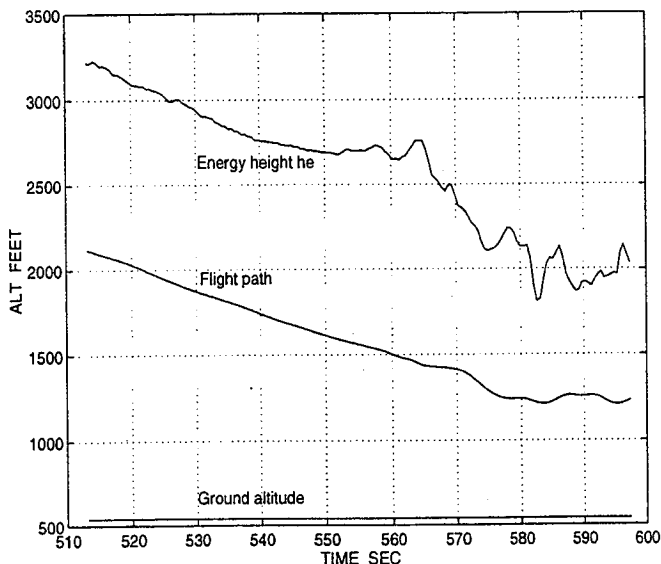


Fig. 10 Altitude in 12-deg pitch hold landing abort (DFW).

$$C_m = C_{m0} + C_{m\alpha}\alpha + C_{m_q}(\dot{q} + \dot{q}_g) + C_{m\delta_H}\delta_H + C_{m\delta_e}\delta_e \quad (32)$$

$$\alpha = \tan^{-1} \frac{W + W_x \sin \theta + W_h \cos \theta}{U + W_x \cos \theta - W_h \sin \theta} \quad (33)$$

$$q_g = \frac{dW_h}{dx} = \frac{\dot{W}_h}{V_x} \quad (34)$$

$$\bar{q} = \frac{1}{2} \rho V^2 \quad (35)$$

$$V = [(W + W_x \sin \theta + W_h \cos \theta)^2 + (U + W_x \cos \theta - W_h \sin \theta)^2]^{1/2} \quad (36)$$

Starting with the correct initial conditions, integration of the previous equations forward in time using the pilot's inputs as recorded on the DFDR, yields the state variables from which the flight path may be obtained. The simulated and recorded flight path and other variables such as airspeed, pitch attitude, and angle of attack were compared. The little discrepancy verified the accuracy of the simulation model.

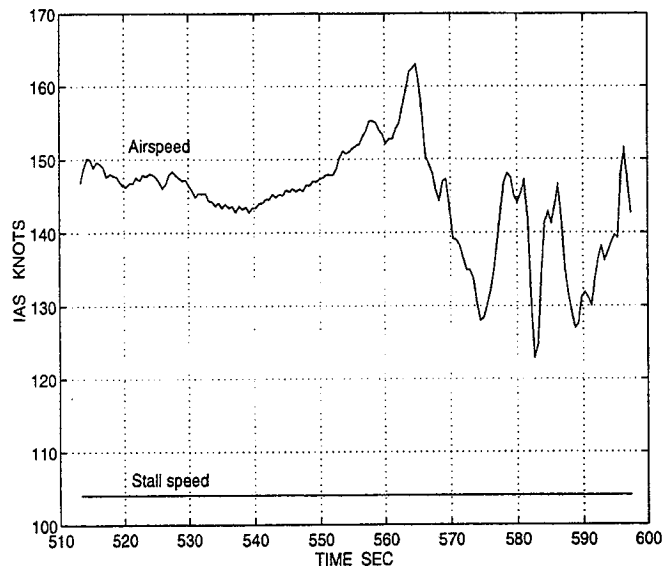


Fig. 11 IAS in 12-deg pitch hold landing abort (DFW).

where U and W are ground referenced inertial velocity components along the body axis, and θ and q are the pitch attitude and pitch rate in the Earth-fixed frame. After substituting C_L , C_D , and C_m into the expanded form of X , Z , and M , the simulation model for the airplane is as follows¹⁰:

$$\dot{U} = (1/m)[(C_L \sin \alpha - C_D \cos \alpha)\bar{q}S + X_T] - g \sin \theta - qW \quad (26)$$

$$\dot{W} = (-1/m)[(C_L \cos \alpha - C_D \sin \alpha)\bar{q}S + Z_T] + g \cos \theta + qU \quad (27)$$

$$\dot{q} = (C_m \bar{q} S \bar{c} + M_T)/I_{yy} \quad (28)$$

$$\dot{\theta} = q \quad (29)$$

where, considering the gust effect on α , q , and airspeed, V ,⁹

$$C_L = C_{L\alpha}(\alpha - \alpha_0) + C_{L\delta_H}\delta_{H_{total}} + C_{L_q}(\dot{q} + \dot{q}_g) + C_{L\dot{\alpha}}\dot{\alpha} \quad (30)$$

$$C_D = C_{D0} + kC_L^2 + C_{D\delta_H}\delta_{H_{total}} \quad (31)$$

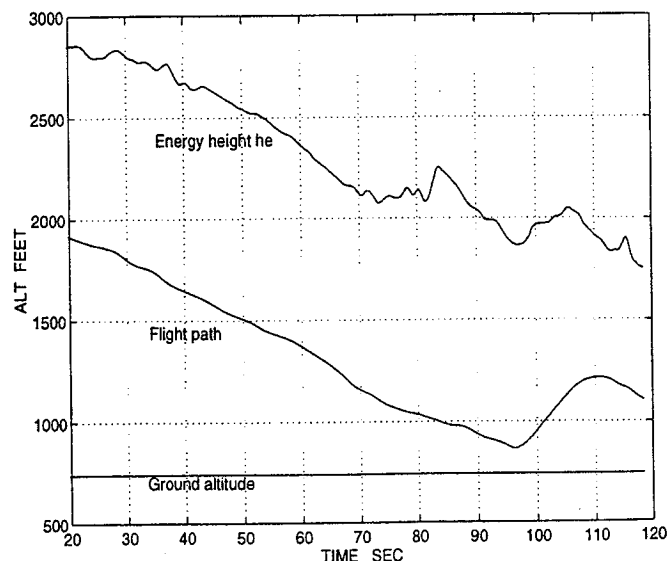


Fig. 12 Altitude in 12-deg pitch hold landing abort (Charlotte).

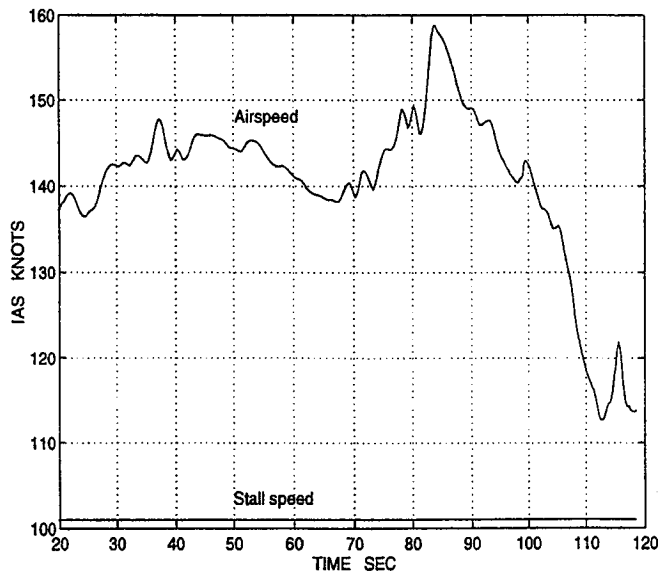


Fig. 13 IAS in 12-deg pitch hold landing abort (Charlotte).

B. Previous Studies

Previous studies of landing abort strategies have been made. Some of these studies have used potential flow to represent the downburst winds.¹¹ Such potential flow models would, for example, poorly represent the DFW downburst where the entrained vortices, which were not included in the model, were a major contributor to the accident. In 1987, Bryson and Zhao proposed a control strategy that allowed satisfactory penetration of a Boeing 727 through a severe downburst during take-off.¹² The strategy used a combination of tight climb-rate hold feedback and full throttle. They used with success Boeing's recommendation for the B-727 of holding a constant pitch attitude of $\theta = 15$ deg while traversing the downburst.

C. Pitch-Hold Landing Abort

In this article, several landing abort strategies were studied for the two downburst encounters. The wind inputs were those of the derived winds that included the entrained vortices. It was assumed that during the landing abort the winds were those affecting the accident airplane. Usually the abort altitude, at a given time, would be greater than that of the accident aircraft for which the winds were known. Consequently, since the horizontal wind gradients decrease with altitude, the present landing abort studies would, in general, be conservative with respect to the degrading effects of the downburst winds.

With respect to the landing abort strategies studied, it was concluded that the most acceptable strategy was to apply maximum thrust and hold constant pitch attitude during the abort. For both the DFW and Charlotte cases a pitch hold of 12 deg appeared to be preferable to 15 deg, the preference being based on the margin of airspeed above the stall.

Figures 10 and 11 show the altitude and airspeed during a simulated landing abort of the L-1011. The abort was started 23 s before impact, with the application of full engine thrust and a 12-deg pitch attitude hold. Figures 12 and 13 show the results of a landing abort of the Charlotte DC-9. The pitch attitude was held constant at 12 deg and throttle was set for maximum climb thrust. The abort was started 23 s before im-

pact. In both abort cases satisfactory altitude and airspeed were maintained.

VI. Conclusions

The wind components along the flight path were first determined and when plotted in vector form displayed the salient characteristics of a downburst. The aircraft, in both cases, upon exiting the downbursts, encountered vortices entrained in the outflow. In the DFW case the vortex was very intense and became a major contributor to the accident.

To quantitatively measure the wind-induced performance degradation, the F -factor and its two components, F_1 and F_2 , were calculated. When plotted in component form, it was shown that, in both cases, F_1 was much larger than F_2 . Consequently, the rapid shift from a headwind to a tailwind, as quantified by F_1 , was the major contributor to the accidents.

Among the many simulations studied of landing aborts, it was concluded that the most acceptable strategy was one of holding constant pitch attitude while having the engines set at maximum climb thrust.

Acknowledgments

This research was made possible by the support of NASA Ames Research Center through Cooperative Agreement NCC-2-329. This support was greatly appreciated. Also, thanks are extended to all the members of the NASA Ames Navigation and Guidance Branch involved in this research.

References

- ¹Bowles, R. L., and Targ, R., "Windshear Detection and Avoidance: Airborne System Perspective," *Proceedings of the 16th Congress of the International Council of the Aeronautical Sciences*, 1988, pp. 7-20.
- ²Stack, D. T., "Turbulence Avoidance," *Proceedings of the 4th International Conference on Aviation Weather Systems*, American Meteorology Society, Boston, MA, 1991, pp. 283-286.
- ³Fujita, T. T., "The Downburst: Microburst and Macrobust," Satellite and Mesometeorology Research Project, Research Paper 210, Univ. of Chicago, Chicago, IL, 1985.
- ⁴Parks, E. K., Bach, R. E., Jr., and Wingrove, R. C., "Analysis of the Nature and Cause of Turbulence Upset Using Airline Flight Records," *Proceedings of the 13th Annual Symposium of the Society of Flight Test Engineers* (New York), Society of Flight Test Engineers, Lancaster, CA, 1982, pp. 151-158.
- ⁵Parks, E. K., Wingrove, R. C., Bach, R. E., Jr., and Mehta, R. S., "Identification of Vortex-Induced Clear Air Turbulence Using Airline Flight Records," *Journal of Aircraft*, Vol. 22, No. 2, 1985, pp. 124-129.
- ⁶Bach, R. E., and Wingrove, R. C., "The Analysis of Airplane Flight Records for Winds and Performance with Application to the Delta 191 Accident," Atmospheric Flight Mechanics Conf., Aug. 1986.
- ⁷Fujita, T. T., "DFW Microburst," Univ. of Chicago, Satellite and Mesometeorology Research Project (SMRP), Chicago, IL, 1986.
- ⁸Etkin, B., *Dynamics of Flight*, Wiley, New York, 1982.
- ⁹Shen, J., "An Analysis of Two Downburst Related Aircraft Accidents," M.S. Thesis, Univ. of Arizona, Tucson, AZ, 1995.
- ¹⁰Aksteter, J. W., Parks, E. K., and Bach, R. E., Jr., "Parameter Identification and Modeling of Longitudinal Aerodynamics," *Journal of Aircraft*, Vol. 32, No. 4, 1995, pp. 726-731.
- ¹¹Zhu, S., "Fluid-Dynamic Model of a Downburst," Univ. of Toronto, UTIAS Rept. 271, Toronto, ON, Canada, 1983.
- ¹²Bryson, A., and Zhao, Y., "Feedback Control for Penetrating a Downburst," *AIAA Guidance and Control Conference* (Monterey, CA), AIAA, New York, 1987.